CONSEJO SUPERIOR DE INVESTIGACIONES
Revista de Investigación de Física. Vol. 8 N° 2 (2005) 14-18
ISSN 1605-7744

NITROGEN INCORPORATION INTO HARD FLUORINATED CARBON FILMS: NANOSCALE FRICTION AND STRUCTURAL MODIFICATIONS

C.M. Sanchez T.[a*], M.E.H. Maia da Costa[a], and F.L. Freire Jr[a]

[A]*Departamento de Física, Pontifícia Universidade Católica do Rio de Janeiro. Cx. Postal 3807, Rio de Janeiro, RJ, 22453-970, Brazil*

Abstract

The nitrogen incorporation into hard fluorinated carbon films deposited by rf-plasma decomposition of CH_4-CF_4-N_2 mixtures was studied. The structural and chemical characterizations of the films were performed by Raman spectroscopy, x-ray photoelectron spectroscopy (XPS) and ion beam analysis. These results show that nitrogen incorporation occurs at the expenses of the carbon content of the films and that it results in an increase of the size and the number of the graphitic domains. XPS spectra show the existence of nitrogen incorporated both into aromatic rings and as terminator radicals. The friction behavior of the films was investigated by atomic force microscopy. The importance of the nitrogen incorporation to surface hidrofobicity and friction processes that occur at nanoasperity contact was verified.

keywords: Raman spectroscopy, X-ray photoelectron spectroscopy, films nanoscale

Resumen

La incorporación del nitrógeno en películas duras de carbono fluorado, depositadas por la descomposición de un plasma de radio frecuencia en un ambiente de CH_4-CF_4-N_2, fue estudiada. Las características estructurales y químicas de las películas fueron realizadas por espectroscopia Raman, espectroscopia fotoelectronica inducida por rayos X (XPS) y análisis por haz de iones. Estos resultados demuestran que la incorporación de nitrógeno ocurre a costas del contenido de carbono en las películas y que da lugar a un aumento del tamaño y del número de los dominios grafíticos. Los espectros de XPS demuestran la existencia de nitrógeno incorporado, ambos en los anillos aromáticos y como radicales terminales. El comportamiento de la fricción de las películas fue investigado por microscopia de fuerza atómica. La importancia de la incorporación de nitrógeno para la hidrofobicidad superficial y los procesos de fricción que ocurren por fuerte contacto a escala nanoscópica, fue verificada.

PACS: 36.20.Ng; 78.30.-j; 79.60.-i; 82.80.Nj
Palabras claves: Espectroscopia Raman, espectroscopia fotoelectrónica inducida por rayos X, películas nanoescalares

1. Introduction

The tribological behavior of moving micro and nanodevices are a challenging subject that impacts their reliabilities and operational lifetimes. The understanding of the fundamental friction and wear processes in nanometer scale is important to achieve such goals [1]. In the last years, many carbon-based protective coatings have been developed. Among these coatings, hydrogenated amorphous carbon films (a-C:H) occupy an important place due to its outstanding properties like high hardness, chemical inertness, high wear resistance and low friction [2].

One controlled way of change the a-C:H film properties is through the incorporation of different elements, like N, F and Si, during the film growth. In spite of the remarkable lubricant properties of poly(tetrafluoroethylene), the recent research on the fluorine incorporation into a-C:H films is mainly motivated by its electrical characteristics. In fact, fluorinated carbon films (a-C:H:F) have been proposed as possible candidates to replace SiO_2 films as interlayer insulators in microelectronic devices due to their low dielectric constant [3]. Notwithstanding the interest on the dielectric properties of fluorinated carbon films, the effect of

* e-mail: sanchez@vdg.fis.puc-rio.br

fluorine incorporation on the mechanical and tribological properties of a-C:H films have not received much attention, despite the substantial friction coefficient reduction that occurs upon fluorine incorporation [4-6]. On the other hand, an important research effort has been dedicated to the study of nitrogen incorporation into a-C:H films during the last decade [7]. The main motivation for these efforts was the intention to synthesize the β-C_3N_4 solid, proposed to have mechanical properties comparable to those of crystalline diamond. Nitrogen incorporation into a-C:H films was found to modify the structure, mechanical and tribological properties [8-10] of these films, as well as their electrical and optical properties [11]. The incorporation of nitrogen into fluorinated carbon films deposited by Plasma Enhanced Chemical Vapor Deposition (PECVD) was also investigated. However, these studies were restricted to the structural characterization and the electrical properties of the films [12-14].

In this work, we present an investigation on the incorporation of N into a-C:H:F films deposited by PECVD using CH_4-CF_4-N_2 mixtures as precursor atmospheres. The effects on the film microstructure and tribological properties will be discussed.

2. Experimental procedures:

The films were deposited by PECVD onto Si substrates mounted on a water-cooled copper cathode fed by a rf (13.56 MHz) power supply. Mixtures of CH_4-CF_4-N_2 were used as precursor atmospheres and the films were deposited at different N_2 partial pressures. The $(CH_4+CF_4)_{x-1}(N_2)_x$ gas mixture was varied from x = 0 to x = 0.65 while the relation CH_4-CF_4 was kept equal to 2:3. The total gas inlet flux was 6sccm. A fixed self-bias of –350V and total pressure of 10Pa were employed and the base pressure was better than 10^{-4}Pa. A 10nm thick a-C:H buffer layer was deposited from pure methane atmosphere in order to improve films adhesion. The initial condition, i.e. x = 0, corresponds to the deposition of hard (12GPa) and dense ($1.3x10^{23}$atoms/cm^3) a-C:H:F films [3].

Ion beam analysis (IBA) was performed in order to determine the films composition while the atomic density was evaluated by combining thickness measurements with the areal atomic density provided by IBA. Details of IBA characterization were published before [4,15].

The chemical bonds were investigated by X-ray photoelectron spectroscopy (XPS). The carbon and nitrogen regions were investigated using a Mg K_α (1253.6eV) x-ray source and a hemispheric analyzer CLAM4 from VG Instruments. The angle between surface normal and the electron energy analyzer axis was 60°.

The atomic arrangement of the films was probed by Raman scattering spectroscopy measurements that were performed with a Renishaw 2000 system using an Ar^+-ion laser (λ = 514nm) in backscattering geometry. The laser power on the sample was ~10mW and the laser spot diameter was 2-3μm. Hydrofobicity was determined by contact angle measurements that were carried out with a Ramé-Hart goniometer and two different droplet sizes of distilled water. The contact angles correspond to an average of ten independent measurements.

The friction measurements were carried out using a Nanoscope IIIa Atomic Force Microscope (AFM) from Digital Instruments in the lateral force regime and performed under controlled ambient conditions. The room temperature was 23°C and the relative humidity ranged from 1 to 55%. The cantilever normal force was obtained by multiplying the measured cantilever bending by its normal bending constant. In order to obtain the absolute values of the friction coefficients, the cantilever bending constant was calibrated using a previously described procedure [16].

3. Results and discussions:

3.1 Structural and chemical characterization:

The films composition determined by IBA and the deposition rates are presented in Table I as functions of the nitrogen partial pressure in the plasma atmosphere. The results show a systematic reduction of the carbon and hydrogen contents upon nitrogen incorporation. The increase of the nitrogen partial pressure was followed by a drastic reduction of the deposition rate. These results show the same behavior observed for a-C:N:H films [8]. The atomic density of the films decreases upon nitrogen incorporation and it can be explained by the reduction of the mean coordination number, since nitrogen essentially replaces carbon atoms, resulting in materials with lower interconnectivity. The trends here observed are in agreement with those obtained from nitrogen incorporated carbon-fluorine films (a-C:H:F:N) deposited by PECVD in similar conditions [12-14].

The carbon and nitrogen *1s* core levels were investigated by XPS and the spectra are presented in Fig. 1 and 2, respectively. The carbon-carbon and carbon-hydrogen bonds peak at 284.5eV dominates the carbon spectra. This main band has a shoulder at the higher binding energy side. For the a-C:H:F film, this shoulder is composed by two bands: one at 289.5eV, that corresponds to the C-*1s* binding energy of a carbon atom directly bonded to a fluorine atom (C-F), while the band at 286.6eV is related to carbon atoms bonded to another carbon in the neighborhood

of a fluorine atom (C-CF) [17]. The $C\text{-}F_2$ and $C\text{-}F_3$ bands are negligible, confirming the high degree of film interconnectivity. When nitrogen is incorporated, besides the C-CF and the C-F bands, two other bands related to carbon-nitrogen bonds appear. These bands at 285.8eV and 287.3eV can be attributed to sp^2-hybridized carbon atoms bonded to nitrogen inside the aromatic structure and to sp^2-hybridized C in the aromatic ring attached to an electronegative group as $C\text{–}NH_2$ or C≡N, respectively [18]. The increase of the nitrogen content in the film results in an increase of the intensity of these two bands and a small reduction of the relative intensity of both C-CF and C-C bands. The intensity of the C-F band does not present an important change. All spectra have a small oxygen surface contaminant. The position of the C-O peak coincides with the C-N peak at 285.8eV. However, since the spectrum obtained from the a-C:H:F film shows that the C-O peak intensity is negligible, we assumed that the oxygen contamination is not important for the interpretation of the XPS data.

Table I: Film composition, atomic density and deposition rate as functions of the N_2 partial pressure in the plasma atmosphere. The errors on the composition and atomic density are of the order of 10 %.

N_2 partial pressure (%)	Composition (at.%)				Density (10^{23} atoms/cm^3)	Deposition rate (nm/min)
	C	N	F	H		
0	80	-	6	14	1.3	23
15	74	6	6	14	1.2	15
30	70	12	6	12	1.1	11
45	69	14	5	12	1.1	7
60	66	20	5	9	1.1	3

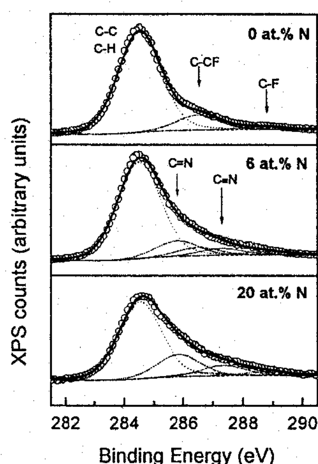

Fig. 1: C-*1s XPS* spectra taken from a-C:H:F:N films with nitrogen content of 0, 6 and 20 at.%. The main features of each spectrum are indicated in the Fig., as well as, the simulated spectra composed by the different bands and the Shirley background.

The nitrogen XPS spectra show in Fig. 2 were fitted with three peaks assigned to nitrogen inside the aromatic structure and bonded to two sp^2-hybridized carbon atoms (398.2eV), N-H bonds (399.1eV) and N≡C (400.2eV) [18,19]. XPS and IBA results suggested that nitrogen atoms replace carbon atoms bonded to hydrogen, while carbon-fluorine bonds are more stable.

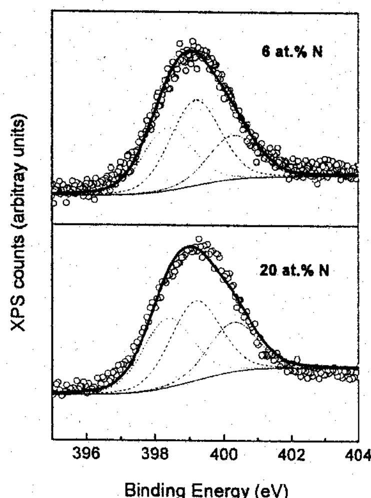

Fig. 2: N-*1s XPS* spectra taken from a-C:H:F:N films with nitrogen content 6 and 20 at.%. The three peaks are assigned to nitrogen inside the aromatic structure and bonded to two sp^2-hybridized carbon atoms (398.2eV), nitrogen-hydrogen bonds (399.1eV) and N≡C (400.2eV). The Shirley background is also shown, as well as, the simulated spectra composed by the different bands

The Raman spectra are shown in Fig. 3. The spectra present only one broad band due to the overlap of the *D* and *G* bands characteristic of amorphous carbon. These peaks were deconvoluted by means of two Gaussian lines. It is clear that microstructure changes occur within nitrogen incorporation. In fact, the *G* band peak position shifts towards higher frequencies (from 1549 to 1565cm^{-1}), accompanied by a reduction of the band width from 135 to 126cm^{-1}, while the I_D/I_G intensity ratio increases by a factor around 2. These results, when obtained from a-C:H films, indicate an increase of the number and size of graphitic domains [20], in agreement with the fact that the incorporation of nitrogen into a-C:H films reduces the fraction of carbon atoms in sp^3 hybridization state [9]. The same interpretation is valid here.

3.2 Nanoscale friction:

Fig. 4 shows the friction force as a function of the normal load for a-C:H:F:N films with a nitrogen

content of 14 at.%. The measurements were performed at relative humidity of 1, 20 and 55%. Within experimental errors, we cannot distinguish these curves. The adhesion forces, determined from the extrapolation to zero of the lateral force was also independent on the relative humidity and, in this case, is 26nN. As shown before, in the low load regime, i.e., in a regime where wear and plastic deformations can be neglect, the friction force did not follow a direct dependence with the applied load [21]. It was shown that friction is proportional to the contact area and that the shear stress was constant within the applied pressure, leading to a $F_F \sim F_L^{2/3}$ dependence of the measured frictional forces. The results presented in Fig. 4 suggested that single-asperity contact mechanical models are valid for the description of our friction data [21]. Similar results and the independence with the ambient conditions were obtained from the other a-C:H:F:N films, as well as, from the a-C:H and a-C:H:F films.

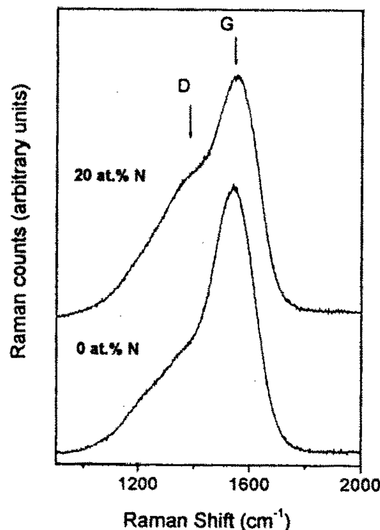

Fig. 3: Raman spectra obtained from a a-C:H:F film and a a-C:H:F:N film with 20 at.% of nitrogen. Arrows indicate the positions of the D and G bands in the spectrum of the a-C:H:F:N film.

In Fig 5 we show the importance of the surface wettability on the friction behavior. In this figure, the friction coefficients and the contact angles were plotted as functions of the nitrogen content in the films. It is clear from the figure that the friction coefficient and the contact angle have an opposite tendency. In a previous publication, it has been shown the same direct correlation between friction forces measured by AFM and the contact angles of a-C:H:F films. [22]. The friction results can be interpreted as been due to the kinetics of nucleation of water meniscus between the moving parts: higher the surface hidrofobicity, less important is the water vapor condensation for the nanoscale friction process [23].

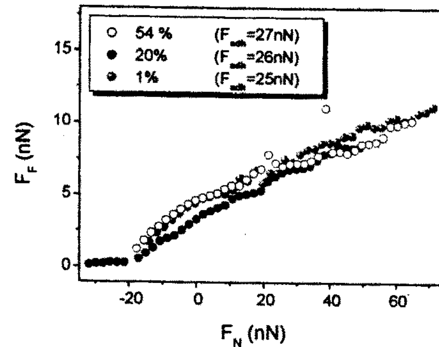

Fig. 4: Friction force as a function of the normal load determined for three values of the relative humidity: 1, 20 and 55%. The adhesion forces are also indicated in the figure. The a-C:H:F:N film has 14 at.% of nitrogen.

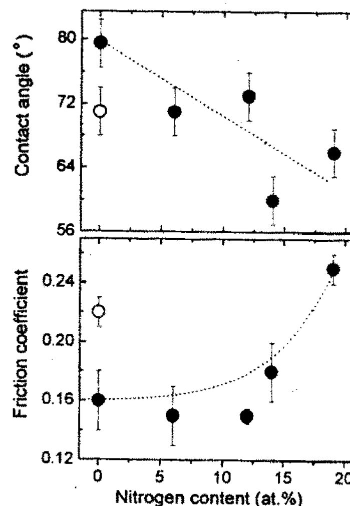

Fig. 5: Contact angle (upper part) and friction coefficient (lower part) as functions of the nitrogen content in the films. The a-C:H:F:N films were represented by black dots, while the open dots correspond to values measured in a-C:H films deposited in pure methane atmosphere (V_b = -350V, P = 10Pa).

4. Summary and conclusions:

In this work, the structural modifications and the nanoscale friction behavior of a-C:H:F:N films are presented. The incorporation of nitrogen, which essentially occurs at the expenses of carbon atoms, increases the number and the size of the graphitic domains as revealed by Raman results. XPS spectra

show that nitrogen atoms are incorporated into the aromatic rings and as electronegative groups directly bonded to sp^2-carbon. The incorporation of nitrogen also induces modifications on the surface hidrofobicity and friction behavior of the films. The observed correlation between the contact angle and the friction coefficient reinforced the importance of the capillary condensation kinetics in the friction process that occurs at nanometer scale.

Acknowledgements:

This work is partially supported by FAPERJ, CAPES and CNPq.

References:

[1]. *Handbook of Micro/NanoTribology*, B. Bushan (Ed.), second edition, CRC Press, Boca Raton, 1999.
[2]. J. Robertson, Prog. Solid State Chem. 21 (1991) 199.
[3]. J.A. Theil, J. Vac. Sci. Technol. B 17 (1999) 2397.
[4]. L.G. Jacobsohn, D.F. Franceschini, M.E.H. Maia da Costa, F.L. Freire Jr., J. Vac. Sci. Technol. A 18 (2000) 2230.
[5]. C. Donnet, J. Fontaine, A. Grill, V. Patel, C. Janhes, M. Belin, Surf. Coat. Technol. 94-95 (1997) 531.
[6]. M. Hakovirta, D.H. Lee, X.M. He, M. Nastasi, J. Vac. Sci. Technol A 19 (2001) 782.
[7]. S. Muhl, J.M. Mendez, Diamond Relat. Mater. 8 (1999) 1809.
[8]. D.F. Franceschini, C.A. Achete, F.L. Freire Jr., Appl. Phys. Lett. 60 (1992) 3229.
[9]. D.F. Franceschini, F.L. Freire Jr., S.R.P. Silva, Appl. Phys. Lett. 68 (1996) 2645.
[10]. R. Prioli, S.I. Zanette, A.O. Caride, F.L. Freire Jr., D.F. Franceschini, J. Vac. Sci. Technol. A 14 (1996) 2351.
[11]. S.R.P. Silva, J. Robertson, G.A.J. Amaratunga, B. Raferty, L.M. Brown, J. Schwan, D.F. Franceschini, G. Mariotto, J. Appl. Phys. 81 (1997) 2626.
[12]. K. Endo, T. Tatsumi, Appl. Phys. Lett. 68 (1996) 3656.
[13]. H. Yokomichi, A. Masuda, J. Non-Cryst. Solids 271 (2000) 147.
[14]. L. Valentini, J.M. Kenny, R.M. Montereali, L. Lozzi, R. Santucci, J. Vac. Sci. Technol. A 20 (2002) 1210.
[15]. F.L. Freire Jr., D.F. Franceschini, C.A. Achete, Nucl. Instrum. Meth. B 85 (1994) 268.
[16]. R. Prioli, A.M. F.Rivas, F.L. Freire Jr., A.O. Caride, Appl. Phys. A 76 (2003) 565-569.
[17]. S. Agraharam, D.H. Hess, P.A. Kohl, S. Bistrup Allen, J. Vac. Sci. Technol. A 17 (1999) 3265.
[18]. J.C. Sanchez-Lopez, C. Donnet, F. Lefèbvre, C-Fernández-Ramos, A. Fernández, J. Appl. Phys. 90 (2001) 675.
[19]. S. Souto, F. Alvarez, Appl. Phys. Lett. 70 (1997) 1539.
[20]. R.O. Dillon, J.A. Woolan, Phys Rev B 29 (1984) 3482.
[21]. U.D. Schwarz, O. Zwöner, P. Köster, R. Wiesendanger, Phys. Rev. B 56 (1997) 6987.
[22]. R. Prioli, L.G. Jacobsohn, M.E.H. Maia da Costa, F.L. Freire Jr., Tribol. Lett. (2003).
[23]. E. Riedo, F. Lévy , H. Brune, Phys. Rev. Lett. 88 (2002) 185505-1.